

## Article

# Synthesis of Elements in Compact Stars in Pycnonuclear Reactions with Carbon Isotopes: Quasibound States vs. States of Zero-Points Vibrations

Sergei P. Maydanyuk <sup>1,\*</sup> , Gyorgy Wolf <sup>1</sup>  and Kostiantyn A. Shaulsky <sup>2</sup><sup>1</sup> Wigner Research Centre for Physics, 1121 Budapest, Hungary; wolf.gyorgy@wigner.hu<sup>2</sup> Institute for Nuclear Research, National Academy of Sciences of Ukraine, 03680 Kyiv, Ukraine; shaulskyi@kinr.kiev.ua

\* Correspondence: sergei.maydanyuk@wigner.hu; Tel.: +36-20-554-5077

**Abstract:** (1) Purpose: Conditions of formation of compound nuclear systems needed for synthesis of heavy nuclei in pycnonuclear reactions in compact stars are studied on a quantum mechanical basis. (2) Methods: The method of multiple internal reflections is applied for pycnonuclear reactions in compact stars with new calculations of quasibound spectra and spectra of zero-point vibrations. (3) Results: Peculiarities of the method are analyzed for reaction with isotopes of Carbon. The developed method takes into account continuity and conservation of quantum flux (describing pycnonuclear reaction) inside the full spacial region of reaction, including the nuclear region. This gives the appearance of new states (called quasibound states) in which compound nuclear systems of Magnesium are formed with the largest probability. These states have not been studied yet in synthesis of elements in stars. Energy spectra of zero-point vibrations and spectra of quasibound states are estimated with high precision for reactions with isotopes of Carbon. For the first time, the influence of plasma screening on quasibound states and states of zero-point vibrations in pycnonuclear reactions has been studied. (4) Conclusions: The probability of formation of a compound nucleus in quasibound states in pycnonuclear reaction is essentially larger than the probability of formation of this system in states of zero-point vibrations studied by Zel'dovich and followers. Therefore, synthesis of Magnesium from isotopes of Carbon is more probable through the quasibound states than through the states of zero-point vibrations in compact stars. Energy spectra of zero-point vibrations are changed essentially after taking plasma screening into account. Analysis shows that from all studied isotopes of Magnesium, only <sup>24</sup>Mg is stable after synthesis at an energy of relative motion of 4.881 MeV of the incident nuclei <sup>12</sup>C.

**Keywords:** pycnonuclear reaction; compact star; neutron star; multiple internal reflections; coefficients of penetrability and reflection; fusion; quasibound state; energy of zero-point vibrations; compound nucleus; dense nuclear matter; tunneling



**Citation:** Maydanyuk, S.P.; Wolf, G.; Shaulsky, K.A. Synthesis of Elements in Compact Stars in Pycnonuclear Reactions with Carbon Isotopes: Quasibound States vs. States of Zero-Points Vibrations. *Universe* **2023**, *9*, 354. <https://doi.org/10.3390/universe9080354>

Academic Editors: Máté Csanád, Péter Kovács, Sándor Lökös and Dániel Kincses

Received: 4 June 2023

Revised: 22 July 2023

Accepted: 24 July 2023

Published: 29 July 2023



**Copyright:** © 2023 by the authors. Licensee MDPI, Basel, Switzerland. This article is an open access article distributed under the terms and conditions of the Creative Commons Attribution (CC BY) license (<https://creativecommons.org/licenses/by/4.0/>).

## 1. Introduction

The phenomenon of nuclear burning occurs in the cold and dense cores of white dwarfs [1] and crusts of neutron stars [2,3]. Such a phenomenon, known as a pycnonuclear reaction [4], is a reaction at sufficiently high densities in stars where zero-point vibrations of nuclei in the lattice sites lead to an essential increasing rate of formation of more heavy nuclei. Insight into this phenomenon was provided by Zel'dovich, who estimated zero-point energy as the energy of the ground state of the harmonic oscillator potential, which is formed near the middle point between two nuclei located in lattice sites [5]. Rates of reactions at such zero-point energies are calculated for some nuclei in compact stars [6].

Fusion is the key process in pycnonuclear reactions. In this process, a new nucleus with a larger mass is produced from the two closest nuclei in the lattice sites. This

question was analyzed for reactions with nuclei of different charges and masses [7]. In that paper, the authors calculated the astrophysical  $S$ -factors for Carbon–Oxygen and Oxygen–Oxygen fusion reactions, wherein a microscopic basis was used. In Ref. [8],  $S$ -factors were calculated for 946 fusion reactions including stable and neutron-rich isotopes of C, O, Ne, and Mg at energies in the range of 2 to  $\approx 18$ –30 MeV. Results in that paper can be converted to thermonuclear or pycnonuclear reaction rates to simulate stellar burning at high temperatures and nucleosynthesis in high-density environments. A large collection of astrophysical  $S$ -factors and their compact representation for isotopes of Be, B, C, N, O, F, Ne, Na, Mg, and Si were presented in Ref. [9]. Finally, a large database of  $S$ -factors was formed for about 5000 nonresonant fusion reactions. The structure of the multi-component matter (a regular lattice, a uniform mix, etc.) in these reactions, plasma screening [10], and rates of reactions in a wide range of temperatures and stellar densities [7,11] have been studied by many researchers.

It has been known that cross-sections of reactions are essentially changed after taking conservation of quantum fluxes into account in the internal region of the nuclear system [12–14]. This question has been studied for  $\alpha$  decays of nuclei and captures of  $\alpha$ -particles by nuclei. For example, nuclear processes during capture before fusion depend on the shape of the nuclear potential [13,14]. Such changes are controlled by additional independent parameters appearing from the fully quantum study. In the fully quantum study, different scenarios of capture (before fusion) can be modelled. Corresponding cross-sections are different by up to four times at the same beam energies of  $\alpha$ -particles in experiments. Often, approaches used with the basis of WKB-approximation neglect these quantum phenomena. It is important to note that this dependence of cross-sections in the fully quantum study is not small. For example, it can be larger essentially than the inclusion of nuclear deformations to the calculation of cross-sections without such quantum parameters. Up to now, the method in Ref. [13] has been the most accurate for the description of experimental data for  $\alpha$ -capture (this calculation is in Figure 3b in Ref. [14] for  $\alpha + {}^{44}\text{Ca}$  in comparison with experimental data [15]).

In the fully quantum study, the accuracy of the determination of penetrability of the barrier and cross-section is about  $10^{-14}$ , while such an accuracy in the WKB-approximation is about  $10^{-1}$ – $10^{-3}$  [13,14]. Pycnonuclear processes are at essentially low energies. In this situation, deep tunneling under the barrier exists only where the semiclassical approximation is not applicable [16]. This indicates the importance of developing fully quantum methods outside of semiclassical approximations. These quantum effects have not been studied yet by other researchers for pycnonuclear reactions in stars. In Ref. [17], investigation of these questions on the fully quantum basis was initiated, for example, for the reaction of  ${}^{12}\text{C} + {}^{12}\text{C}$ . The interest in that reaction is explained by its impact on nucleosynthesis, energy production, and other questions in stellar evolution [11,18]. In addition, this reaction has a significant impact on the evolution and structure of massive stars with  $M \geq M_{\odot}$  ( $M_{\odot}$  is the Solar mass).  ${}^{12}\text{C} + {}^{12}\text{C}$  fusion is known as a pycnonuclear reaction that reignites a Carbon–Oxygen white dwarf into a type Ia supernova explosion. However, it could be useful to obtain a more complete picture for the systematic analysis of nuclear processes and fusion for reactions with isotopes of Carbon. Therefore, in this paper, we perform such an investigation for pycnonuclear reactions with Carbon.

The paper is organized in the following way. In Section 2, a new generalized formalism of the multiple internal reflections is reviewed with focus on new elements for fusion and quasibound states in pycnonuclear reactions. In Section 3, reactions with isotopes of Carbon on the basis of the method are studied using calculations of penetrabilities of the potential barriers, probabilities of formation of the compound nucleus, estimation of energies for zero-point vibrations and quasibound states, etc. In Section 4, the influence of plasma screening on properties of the pycnonuclear reaction is studied in the example of  ${}^{12}\text{C} + {}^{12}\text{C}$ . Conclusions are summarized in Section 6.

## 2. Method of Quantum Mechanics for Nucleus–Nucleus Scattering with Fusion

We will study the capture of one nucleus with smaller mass by another nucleus with larger mass. This process can be studied on the basis of the solution of the Schrödinger equation with radial potential, which has a barrier approximated by a large number  $N$  of rectangular steps:

$$V(r) = \begin{cases} V_1 & \text{at } r_{\min} < r \leq r_1 & \text{(region 1),} \\ \dots & \dots & \dots \\ V_{N_{\text{cap}}} & \text{at } r_{N_{\text{cap}}-1} \leq r \leq r_{\text{cap}} & \text{(region } N_{\text{cap}}), \\ \dots & \dots & \dots \\ V_N & \text{at } r_{N-1} \leq r \leq r_{\max} & \text{(region } N), \end{cases} \quad (1)$$

where  $V_j$  are constants ( $j = 1 \dots N$ ).  $r_1 \dots r_N$  are parameters of the discretization scheme with constant step used in computer calculations. One can calculate these parameters as follows:

$$\begin{aligned} \Delta r &= \frac{r_{\max} - r_{\min}}{N}, \\ r_1 &= \Delta r \cdot 1 + r_{\min}, & r_{N-1} &= \Delta r \cdot (N - 1) + r_{\min}, \\ r_2 &= \Delta r \cdot 2 + r_{\min}, & r_N &= \Delta r \cdot N + r_{\min} = r_{\max}. \\ r_i &= \Delta r \cdot i + r_{\min}, \end{aligned} \quad (2)$$

The solution of the radial wave function for the above barrier energies is:

$$\chi(r) = \begin{cases} \alpha_1 e^{ik_1 r} + \beta_1 e^{-ik_1 r}, & \text{at } r_{\min} < r \leq r_1, \\ \alpha_2 e^{ik_2 r} + \beta_2 e^{-ik_2 r}, & \text{at } r_1 \leq r \leq r_2, \\ \dots & \dots \\ \alpha_{N-1} e^{ik_{N-1} r} + \beta_{N-1} e^{-ik_{N-1} r}, & \text{at } r_{N-2} \leq r \leq r_{N-1}, \\ e^{-ik_N r} + A_R e^{ik_N r}, & \text{at } r_{N-1} \leq r \leq r_{\max}, \end{cases} \quad (3)$$

where  $\alpha_j$ ,  $\beta_j$ , and  $A_R$  are unknown amplitudes and  $k_j = \frac{1}{\hbar} \sqrt{2m(\tilde{E} - V_j)}$  are wave numbers. We will present the solution of this problem on the basis of the method of multiple internal reflections (see Refs. [19,20], references therein).

Note that, previously, the process of the capture of  $\alpha$ -particles on nuclei was studied by us in Ref. [13], where we presented details of our formalism, demonstrated its accuracy in comparison with other existing methods, and used tests to check calculations. However, in Ref. [13], it was not taken into account that after tunneling through the barrier, further propagation of waves inside the internal region of potential exists. This aspect requires important modification of the formalism and estimations that were studied in Ref. [14]. In the current paper, we use results of the study in Ref. [14]. According to that research, we will indicate the region with the number  $N_{\text{capture}}$  as the place where the capture of the particle by the nucleus takes place with the largest probability.

In each region of potential, we calculate summed amplitudes as:

$$\tilde{T}_{j-1}^- = \frac{\tilde{T}_j^- T_{j-1}^-}{1 - R_{j-1}^- \tilde{R}_j^+}, \quad \tilde{R}_{j-1}^+ = R_{j-1}^+ + \frac{T_{j-1}^+ \tilde{R}_j^+ T_{j-1}^-}{1 - \tilde{R}_j^+ R_{j-1}^-}, \quad \tilde{R}_{j+1}^- = R_{j+1}^- + \frac{T_{j+1}^- \tilde{R}_j^- T_{j+1}^+}{1 - R_{j+1}^+ \tilde{R}_j^-}, \quad (4)$$

where:

$$\begin{aligned} T_j^+ &= \frac{2k_j}{k_j + k_{j+1}} e^{i(k_j - k_{j+1})r_j}, & T_j^- &= \frac{2k_{j+1}}{k_j + k_{j+1}} e^{i(k_j - k_{j+1})r_j}, \\ R_j^+ &= \frac{k_j - k_{j+1}}{k_j + k_{j+1}} e^{2ik_j r_j}, & R_j^- &= \frac{k_{j+1} - k_j}{k_j + k_{j+1}} e^{-2ik_{j+1} r_j}. \end{aligned} \quad (5)$$

All amplitudes  $\tilde{R}_{N-2}^+ \dots \tilde{R}_{N_{\text{cap}}}^+$  and  $\tilde{T}_{N-2}^- \dots \tilde{T}_{N_{\text{cap}}}^-$  are calculated on the basis of these recurrent relations, above where at the start one can use:

$$\tilde{R}_{N-1}^+ = R_{N-1}^+, \quad \tilde{T}_{N-1}^- = T_{N-1}^- \tag{6}$$

On the basis of such amplitudes, we calculate summed amplitudes  $\alpha_j$  and  $\beta_j$  as:

$$\beta_j \equiv \sum_{i=1} \beta_j^{(i)} = \frac{\tilde{T}_j^-}{1 - \tilde{R}_{j-1}^- \tilde{R}_j^+}, \quad \alpha_j \equiv \sum_{i=1} \alpha_j^{(i)} = \frac{\tilde{R}_{j-1}^- \tilde{T}_j^-}{1 - \tilde{R}_{j-1}^- \tilde{R}_j^+} \tag{7}$$

Summed amplitude  $A_{T,\text{bar}}$  of transition through the barrier or summed amplitude  $A_{R,\text{bar}}$  of reflection from the barrier are determined as all waves transmitted through the potential region with the barrier from  $r_{\text{cap}}$  to  $r_{N-1}$  or reflected from this potential region as:

$$A_{T,\text{bar}} = \tilde{T}_{N_{\text{cap}}}^-, \quad A_{R,\text{bar}} = \tilde{R}_{N-1}^-, \quad \text{at } \tilde{R}_{N_{\text{cap}}}^- = R_{N_{\text{cap}}}^- \tag{8}$$

The method of multiple internal reflections also allows us to determine resonant and potential scatterings. Here, potential scattering can be defined on the basis of summed amplitude  $A_{R,\text{ext}}$  of all waves reflected from the external barrier region, i.e., the region between the external turning point  $r_{\text{tp,ext}}$  and  $r_{N-1}$ , and propagated outside as:

$$A_{R,\text{ext}} = \tilde{R}_{N-1}^-, \quad \text{at } \tilde{R}_{N_{\text{tp,ext}}}^- = R_{N_{\text{tp,ext}}}^- \tag{9}$$

Resonant scattering can be defined on the basis of the summed amplitude  $A_{R,\text{tun}}$  of all waves that are reflected from the potential region between point  $r_{\text{cap}}$  and the external turning point  $r_{\text{tp,ext}}$  as:

$$A_{R,\text{tun}} = A_{R,\text{bar}} - A_{R,\text{ext}} \tag{10}$$

The coefficient of penetrability  $T_{\text{bar}}$  and the coefficient of reflection  $R_{\text{bar}}$  concerning the potential barrier region, the coefficient  $R_{\text{ext}}$  of reflection from the external part of the barrier, and the coefficient  $R_{\text{tun}}$  of reflection from the pure barrier region are defined as:

$$T_{\text{bar}} = \frac{k_{\text{cap}}}{k_N} \|A_{T,\text{bar}}\|^2, \quad R_{\text{bar}} = \|A_{R,\text{bar}}\|^2, \quad R_{\text{ext}} = \|A_{R,\text{ext}}\|^2, \quad R_{\text{tun}} = \|A_{R,\text{tun}}\|^2 \tag{11}$$

A useful characteristic is amplitude of oscillations, defined concerning the point of capture with the number  $N_{\text{cap}}$  as:

$$A_{\text{osc}}(N_{\text{cap}}) = \frac{1}{1 - \tilde{R}_{N_{\text{cap}}-1}^- \tilde{R}_{N_{\text{cap}}}^+} \tag{12}$$

In the standard test of quantum mechanics:

$$T_{\text{bar}} + R_{\text{bar}} = 1 \tag{13}$$

is naturally used in the formalism of multiple internal reflections.

According to the formalism of the method of multiple internal reflections [17], the probability of the existence of a compound nucleus is defined, as the integral over the region between two internal turning points, as:

$$P_{\text{cn}} \equiv \int_{r_{\text{int}1}}^{r_{\text{int}2}} \|\chi(r)\|^2 dr = \sum_{j=1}^{n_{\text{int}}} \left\{ (\|\alpha_j\|^2 + \|\beta_j\|^2) \Delta r + \frac{\alpha_j \beta_j^*}{2ik_j} e^{2ik_j r} \Big|_{r_{j-1}}^{r_j} - \frac{\alpha_j^* \beta_j}{2ik_j} e^{-2ik_j r} \Big|_{r_{j-1}}^{r_j} \right\} \tag{14}$$

The solutions presented above are essentially simplified for the simplest barrier in Equation (1) in Ref. [14]. We write down  $P_{\text{cn}}(E)$  as in Ref. [14] (see Equations (6) and (7)):

$$\begin{aligned}
 P_{\text{cn}}^{(\text{without fusion})} &= P_{\text{osc}} T_{\text{bar}} P_{\text{loc}}, \\
 P_{\text{osc}} &= \|A_{\text{osc}}\|^2 = \frac{(k + k_1)^2}{2k^2(1 - \cos(2k_1r_1)) + 2k_1^2(1 + \cos(2k_1r_1))}, \\
 T_{\text{bar}} &\equiv \frac{k_1}{k_2} \|T_1^-\|^2, \\
 P_{\text{loc}} &= 2 \frac{k_2}{k_1} \left( r_1 - \frac{\sin(2k_1r_1)}{2k_1} \right).
 \end{aligned}
 \tag{15}$$

For fast fusion for the simplest barrier, we obtain:

$$P_{\text{cn}}^{(\text{fast fusion})} = \left\| \sum_{i=1}^{r_1} \beta_1^{(i)} \right\|^2 \int_0^{r_1} \|R_0 e^{ik_1r} + e^{-ik_1r}\|^2 dr = \|T_1^-\|^2 r_1 = \frac{k_2 r_1}{k_1} T_{\text{bar}}.
 \tag{16}$$

The fusion cross-section  $\sigma$  is defined as (see Ref. [13] for details):

$$\sigma_{\text{fus}}(E) = \sum_{l=0}^{+\infty} \sigma_l(E), \quad \sigma_l = \frac{\pi \hbar^2}{2mE} (2l + 1) f_l(E) P_{\text{cn}}(E).
 \tag{17}$$

Here,  $E$  is the energy of the relative motion between two nuclei,  $\sigma_l$  is the partial cross-section at  $l$ , and  $P$  is the probability of formation of a compound nuclear system as defined in Equation (14) or (16). In this formula, an additional factor  $f_l(E)$  is included, which is needed to connect the old factor of fusion  $P_l$  and the new probability  $P_{\text{cn}}(E)$  and penetrability of the barrier region  $T_{\text{bar},l}(E)$ . This coefficient can be written down in explicit form for complete fusion:

$$f(E) = \frac{k_{\text{cap}}}{k_N \|r_{\text{cap}} - r_{\text{tp,in},1}\|}.
 \tag{18}$$

The formalism developed above allows us to model different scenarios of fusion. For example, for the formation of the compound nucleus with slow fusion (i.e., without instantaneous fusion), we vary fusion coefficients in the region between points  $r_{\text{cap}}$  and  $r_{\text{int},2}$ .

### 3. Analysis

We will study the reactions  ${}^X\text{C} + {}^X\text{C} = {}^{2X}\text{Mg}$  [11] ( $X = 10, 12, 14, 18, 20, 22, 24$ ) in this paper. The first indications of the possibility to synthesize more heavy elements from Carbon isotopes can be found in the research of Hamada and Salpeter [21], based on pycnonuclear reaction rates derived by Cameron [4]. Hamada and Salpeter estimated a density of  $6 \times 10^9 \text{ g} \times \text{cm}^{-3}$  via a pycnonuclear process where nuclei of  ${}^{12}\text{C}$  are transformed into  ${}^{24}\text{Mg}$  at low energies. Then, estimates of densities of the stellar medium for those reactions were improved [1]. Note that there were uncertainties in the estimation of densities in those calculations. Moreover, estimations of rates can be changed to include temperatures and crystal imperfections in analysis. Summarizing, the critical density for Carbon was found to be  $5 \times 10^{10} \text{ g} \times \text{cm}^{-3}$ . We will focus on the understanding of new quantum phenomena, which exist in pycnonuclear reactions and have not been studied yet by other researchers. As the inclusion of such effects can significantly change the rates of reactions and even the picture of participating mechanisms, for brevity of calculations, we will use the density obtained by Hamada and Salpeter for the analysis of isotopes of Carbon.

#### 3.1. Potential of Interaction for Nuclei in Lattice Sites

The potential of interactions between isotopes of Carbon  ${}^X\text{C}$  is defined as:

$$V(r) = v_c(r) + v_N(r) + v_{l=0}(r),
 \tag{19}$$

where  $v_c(r)$ ,  $v_N(r)$ , and  $v_l(r)$  are Coulomb, nuclear, and centrifugal components that have the form:

$$v_N(r) = -\frac{V_R}{1 + \exp\left\{\frac{r - R_R}{a_R}\right\}}, \quad v_l(r) = \frac{l(l+1)}{2mr^2},$$

$$v_c(r) = \begin{cases} \frac{Z_1 Z_2 e^2}{r}, & \text{at } r \geq R_c, \\ \frac{Z_1 Z_2 e^2}{2R_c} \left\{3 - \frac{r^2}{R_c^2}\right\}, & \text{at } r < R_c. \end{cases} \quad (20)$$

Here,  $V_R$  is the strength of the nuclear term, defined as:

$$V_R = -75.0 \text{ MeV}. \quad (21)$$

$R_c$  is the Coulomb radius of the nuclear system,  $R_R$  is the nuclear radius of the nuclear system,  $m$  is the reduced mass defined in Equation (30), and  $a_R$  is the diffusion parameter. We define these parameters as [17,22]:

$$R_R = r_R (A_1^{1/3} + A_2^{1/3}), \quad R_c = r_c (A_1^{1/3} + A_2^{1/3}), \quad a_R = 0.44 \text{ fm},$$

$$r_R = 1.30 \text{ fm}, \quad r_c = 1.30 \text{ fm}. \quad (22)$$

These potentials for isotopes of Carbon are presented in Figure 1.

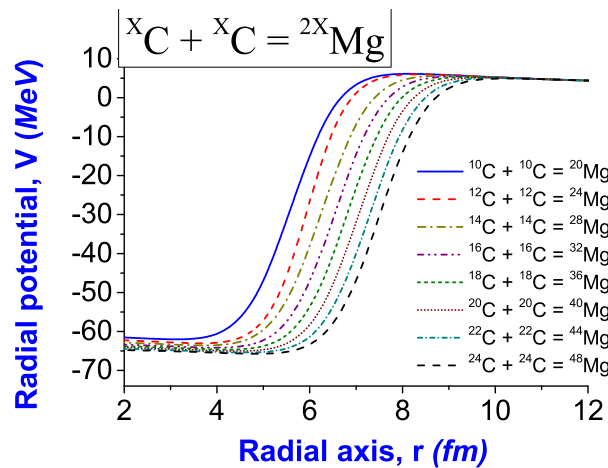


**Figure 1.** Potentials of interaction between two nuclei of Carbon  ${}^X\text{C}$  (potentials and parameters are defined in Equations (19)–(21)).

A small difference between the shapes of the internal wells of the potentials is clearly visible in this figure (this internal well is absent in potentials used in Ref. [6], for example). For brevity, we include maximums of barriers and minimums of wells for potentials of interaction between nuclei in Table 1.

**Table 1.** Minimums of wells and maximums of barriers of potentials of interactions between two isotopes of Carbon, as well as distance  $R_0$  between nuclei and their concentration  $n_A$  (isotopes of Carbon are chosen in accordance with Ref. [8] on the systematic study of astrophysical S-factors in fusion reactions for C, O, Ne, Mg; parameters are determined for density  $\rho_0 = 6 \times 10^9 \frac{\text{g}}{\text{cm}^3}$ ).

Reaction ${}^X\text{C} + {}^X\text{C}$	$r_{\text{min}}, \text{ fm}$	$V_{\text{min}}, \text{ MeV}$	$r_{\text{max}}, \text{ fm}$	$V_{\text{max}}, \text{ MeV}$	$R_0, \text{ fm}$	$n_A, 10^{-7} \text{ fm}^{-3}$
${}^{10}\text{C} + {}^{10}\text{C}$	3.36	−62.157	7.98	+6.249	87.06	3.61702731
${}^{12}\text{C} + {}^{12}\text{C}$	3.64	−63.018	8.33	+5.972	92.52	3.01418941
${}^{14}\text{C} + {}^{14}\text{C}$	3.92	−63.702	8.68	+5.743	97.40	2.58359092
${}^{16}\text{C} + {}^{16}\text{C}$	4.20	−64.258	8.96	+5.552	101.83	2.26064206
${}^{18}\text{C} + {}^{18}\text{C}$	4.48	−64.726	9.24	+5.386	105.91	2.00945961
${}^{20}\text{C} + {}^{20}\text{C}$	4.62	−65.133	9.52	+5.242	109.69	1.80851365
${}^{22}\text{C} + {}^{22}\text{C}$	4.90	−65.483	9.80	+5.115	113.23	1.64410331
${}^{24}\text{C} + {}^{24}\text{C}$	5.04	−65.792	10.08	+5.001	116.57	1.50709470

### 3.2. Space Location of Nuclei in Lattice Sites

Following the logic in Ref. [6] (see p. 90, Figure 3.5 in that book), the distance between the two closest nuclei located in lattice sites is  $2 R_0$ . We place the “incident” nucleus between these nuclei. Such a distance can be derived as:

$$\rho_0 = \frac{m_A}{V_A} = \frac{A m_u}{4/3 \pi R_0^3} \tag{23}$$

or:

$$R_0 = \left( \frac{A m_u}{4/3 \pi \rho_0} \right)^{1/3}. \tag{24}$$

Here,  $\rho_0$  is the density in the sphere surrounding one nucleus of the lattice site,  $V_A$  is the volume inside this sphere,  $A$  is the mass number of the nucleus,  $m_A$  is the mass of the nucleus, and  $m_u$  is the mass of the nucleon. One can calculate the concentration of nuclei  $n_A$  as:

$$n_A = \frac{\rho_0}{A m_u}. \tag{25}$$

For analysis of the pycnonuclear reactions  ${}^X\text{C} + {}^X\text{C} = {}^{2X}\text{Mg}$ , we choose to use the density estimated in Ref. [6]:

$$\rho_0 = 6 \times 10^9 \frac{\text{g}}{\text{cm}^3}. \tag{26}$$

The derived distance  $R_0$  and concentration  $n_A$  for different isotopes of Carbon at such a density are given in Table 1.

### 3.3. Energy Spectra of Zero-Point Vibrations of Nuclei in Lattice Sites

A nucleus located in a lattice site and located between two nuclei with adjacent sites can oscillate and has a discrete spectrum of energy from such oscillations. The approach to determine the energy levels of such a spectrum was investigated by Zel’dovich and other researchers. In this approach, the energy of zero-point vibrations of the nucleus in the lattice site is calculated as [6] (see Equations (3.7.19) and (3.7.20)):

$$E_0^{(\text{zero})} = \frac{\hbar\omega}{2} = \frac{\hbar Ze}{\sqrt{m R_0^3}}, \quad \Delta E = \frac{2 Z^2 e^2}{R_0}, \quad E_{\text{full}} = E_0^{(\text{zero})} + \Delta E. \tag{27}$$

Here,  $E_0^{(\text{zero})}$  is the energy of the ground state of the harmonic oscillator relative to the potential minimum of this oscillator,  $\Delta E$  is the shift of the oscillator relative to the zero value of the potential of interaction between nuclei (i.e., the distance between the minimum of the oscillator and the zero value of the potential of the interaction), and  $E_{\text{full}}$  is the energy value of the ground state in the system relative to the zero value of the potential. For example, for the reaction  ${}^{12}\text{C} + {}^{12}\text{C} = {}^{24}\text{Mg}$ , we obtain:

$$E_0^{(\text{zero})} = 0.02180806 \text{ MeV}, \quad \Delta E = 0.56787237 \text{ MeV}, \quad E_{\text{full}}^{(\text{zero mode})} = 0.58968043 \text{ MeV}. \tag{28}$$

We call such a state the *state of zero-point vibrations of nuclei* (or the *state of zero mode*).

However, the harmonic oscillator has not only the ground state but the full discrete energy spectrum, which is calculated as:

$$E_n^{(\text{zero})} = (2n + 1) \cdot \frac{\hbar\omega}{2} = (2n + 1) \cdot E_{n=0}^{(\text{zero})} = (2n + 1) \frac{\hbar Ze}{\sqrt{m R_0^3}}. \tag{29}$$

The energy spectrum can be written down via density of matter  $\rho_0$  instead of distance  $R_0$ . Using Equation (24) and the formula for reduced mass:

$$R_0 = \left( \frac{A m_u}{4/3 \pi \rho_0} \right)^{1/3}, \quad m = m_p \frac{A_1 A_2}{A_1 + A_2}, \tag{30}$$

from Equation (27), we obtain (let us consider the case of the same nuclei in the lattice:  $A_1 = A_2$ , and  $A = A_1$ ):

$$E_0^{(zero)} = c_1 \cdot \frac{Z}{A} \sqrt{\rho_0}, \quad c_1 = \hbar e \sqrt{\frac{8\pi}{3 m_u m_p}},$$

$$\Delta E = c_2 \cdot Z^2 \left(\frac{\rho_0}{A}\right)^{1/3}, \quad c_2 = 2e^2 \left(\frac{4\pi}{3 m_u}\right)^{1/3}.$$
(31)

We find new interesting property for nuclei of type  $2Z = A$ :

$$E_0^{(zero)} = \frac{c_1}{2} \sqrt{\rho_0}, \quad \Delta E = c_2 \cdot Z^2 \left(\frac{\rho_0}{2Z}\right)^{1/3}.$$
(32)

Thus, according to this property, the spectra  $E_n^{(zero)}$  are the same for nuclei  ${}^8\text{Be}$ ,  ${}^{10}\text{B}$ ,  ${}^{12}\text{C}$ ,  ${}^{14}\text{N}$ ,  ${}^{16}\text{O}$ ,  ${}^{18}\text{F}$ ,  ${}^{20}\text{Ne}$ ,  ${}^{22}\text{Na}$ ,  ${}^{24}\text{Mg}$ ,  ${}^{26}\text{Si}$ , etc. Those depend only on the chosen density in the stellar medium. In Table 2, energy values are presented for the first 10 states of zero-point vibrations calculated by Equation (27) for reactions  ${}^X\text{C} + {}^X\text{C}$ .

**Table 2.** Energy levels for the first 10 states of zero-point vibrations calculated by Equations (27) for reactions  ${}^X\text{C} + {}^X\text{C}$ .

No.	Energy, $E_n^{(zero)}$ , MeV	Energy, $E_{full}^{(zero)}$ , MeV
1	0.021808061833736	0.589680437522993
2	0.065424185501208	0.633296561190465
3	0.109040309168680	0.676912684857937
4	0.152656432836153	0.720528808525410
5	0.196272556503626	0.764144932192882
6	0.239888680171098	0.807761055860354
7	0.283504803838570	0.851377179527827
8	0.327120927506043	0.894993303195299
9	0.370737051173515	0.938609426862772
10	0.414353174840987	0.982225550530244

Energies of states of zero-point vibrations can be reestimated on the basis of the method of multiple internal reflections. For that, let us write down the radial wave function in the asymptotic region:

$$\chi(r) = e^{-ikr} + A_R e^{+ikr}.$$
(33)

Following quantum mechanics, the full wave function should be zero at point  $R_0$  (for odd states) or be maximal in the module at that point (for even states):

$$(1) \quad \chi(R_0) = e^{-ikR_0} + A_R e^{+ikR_0} = e^{-ikR_0} + e^{+ikR_0}, \quad A_R = +1,$$

$$(2) \quad \chi(R_0) = e^{-ikR_0} + A_R e^{+ikR_0} = e^{-ikR_0} - e^{+ikR_0}, \quad A_R = -1.$$
(34)

This requirement gives discreteness of the spectrum of energy for such states. Energy levels can be found if we impose a condition on the imaginary part of such an amplitude to equal zero:

$$\begin{aligned} \text{even states: } & A_R = +1, \quad \text{Re}(A_R) = +1, \quad \text{Im}(A_R) = 0, \\ \text{odd states: } & A_R = -1, \quad \text{Re}(A_R) = -1, \quad \text{Im}(A_R) = 0. \end{aligned}$$
(35)

The energies for states of zero-point vibrations for Carbon isotopes  ${}^X\text{C} + {}^X\text{C} \rightarrow {}^{2X}\text{Mg}$  are given in Table 3.

**Table 3.** Energies of zero-point vibrations  $E_{\text{zero}}^{(\text{mir})}$  for reactions  ${}^X\text{C} + {}^X\text{C}$  (presented data are in MeV, below 5 MeV) calculated by the method of multiple internal reflections (see Section 3.3 for details). Distances between each two adjacent energies are essentially different from the energy spectrum of the harmonic oscillator (see Equation (31), Table 2). There are few energies below the energy of the zero-point vibrations in the ground state  $E_{\text{full},0}^{(\text{zero})}$  derived by the approach of Zel’dovich and his colleagues (see Equation (27)). These energies are derived with accuracy, which can be estimated from condition  $|\text{Re}(A_R)| \approx 1$ . Additional estimation of accuracy of the calculated amplitude can be done by checking the condition of  $[\text{Re}(A_R)]^2 + [\text{Im}(A_{\text{rmR}})]^2 = 1$ . Summation of  $[\text{Re}(A_R)]^2 + [\text{Im}(A_{\text{rmR}})]^2$  is an additional estimation of accuracy for the method of MIR in determination of obtained digits of the amplitude.

No.	${}^{10}\text{C} + {}^{10}\text{C}$	${}^{12}\text{C} + {}^{12}\text{C}$	${}^{14}\text{C} + {}^{14}\text{C}$	${}^{16}\text{C} + {}^{16}\text{C}$
1	0.517434869739479	0.517434869739479	0.517434869739479	0.527054108216433
2	0.536673346693387	0.536673346693387	0.536673346693387	0.536072144288577
3	0.546292585170341	0.546292585170341	0.546292585170341	0.545090180360721
4	0.565531062124249	0.555911823647295	0.555911823647295	0.554108216432866
5	0.584769539078156	0.575150300601202	0.565531062124249	0.572144288577154
6	0.613627254509018	0.594388777555110	0.575150300601202	0.581162324649299
7	0.642484969939880	0.613627254509018	0.594388777555110	0.599198396793587
8	0.680961923847695	0.642484969939880	0.623246492985972	0.626252505010020
9	0.738677354709419	0.680961923847695	0.652104208416834	0.653306613226453
10	0.815631262525050	0.729058116232465	0.690581162324649	0.689378757515030
11	0.950300601202405	0.806012024048096	0.729058116232465	0.734468937875752
12	1.27735470941884	0.911823647294589	0.796392785571142	0.797595190380762
13	2.23927855711423	1.11382765531062	0.892585170340681	0.878757515030060
14	3.69178356713427	2.76833667334669	1.04649298597194	1.02304609218437
15	—	4.08617234468938	1.64288577154309	1.39278557114228
16	—	—	3.04729458917836	1.99699398797595
17	—	—	4.28817635270541	3.20541082164329
18	—	—	—	4.37775551102204
No.	${}^{18}\text{C} + {}^{18}\text{C}$	${}^{20}\text{C} + {}^{20}\text{C}$	${}^{22}\text{C} + {}^{22}\text{C}$	${}^{24}\text{C} + {}^{24}\text{C}$
1	0.517434869739479	0.527054108216433	0.536673346693387	0.517434869739479
2	0.527054108216433	0.546292585170341	0.546292585170341	0.527054108216433
3	0.536673346693387	0.555911823647295	0.555911823647295	0.536673346693387
4	0.546292585170341	0.565531062124249	0.565531062124249	0.584769539078156
5	0.555911823647295	0.584769539078156	0.575150300601202	0.594388777555110
6	0.565531062124249	0.604008016032064	0.594388777555110	0.613627254509018
7	0.575150300601202	0.623246492985972	0.604008016032064	0.632865731462926
8	0.584769539078156	0.642484969939880	0.623246492985972	0.661723446893788
9	0.594388777555110	0.671342685370741	0.652104208416834	0.690581162324649
10	0.613627254509018	0.709819639278557	0.680961923847695	0.729058116232465
11	0.632865731462926	0.748296593186373	0.719438877755511	0.767535070140281
12	0.661723446893788	0.806012024048096	0.757915831663327	0.825250501002004
13	0.738677354709419	0.882965931863727	0.815631262525050	0.911823647294589
14	0.796392785571142	1.00801603206413	0.892585170340681	1.02725450901804
15	0.882965931863727	1.27735470941884	1.01763527054108	1.29659318637275
16	1.00801603206413	2.24889779559118	1.27735470941884	2.20080160320641
17	1.30621242484970	3.26853707414830	2.24889779559118	3.14348697394790
18	2.18156312625251	4.29779559118237	3.22044088176353	4.08617234468938
19	3.26853707414830	—	4.21122244488978	—

### 3.4. Probabilities of Formation of Compound Nuclei in Pycnonuclear Reactions

Our analysis has shown that the coefficients of penetrability and reflection increase monotonously with the energy of the incident nucleus [17]. This means that penetrability and reflection themselves cannot indicate the possible existence of some definite states of more heavy nuclei synthesized in pycnonuclear reactions in stars. Such behavior of

these characteristics is in agreement with the analysis of the capture of  $\alpha$ -particles by nuclei [13,14].

Another important quantum characteristic is the probability of formation of a compound nucleus, which can be created during the studied reactions with nuclei. In Figure 2, we present such probabilities for isotopes of Carbon calculated by our method.

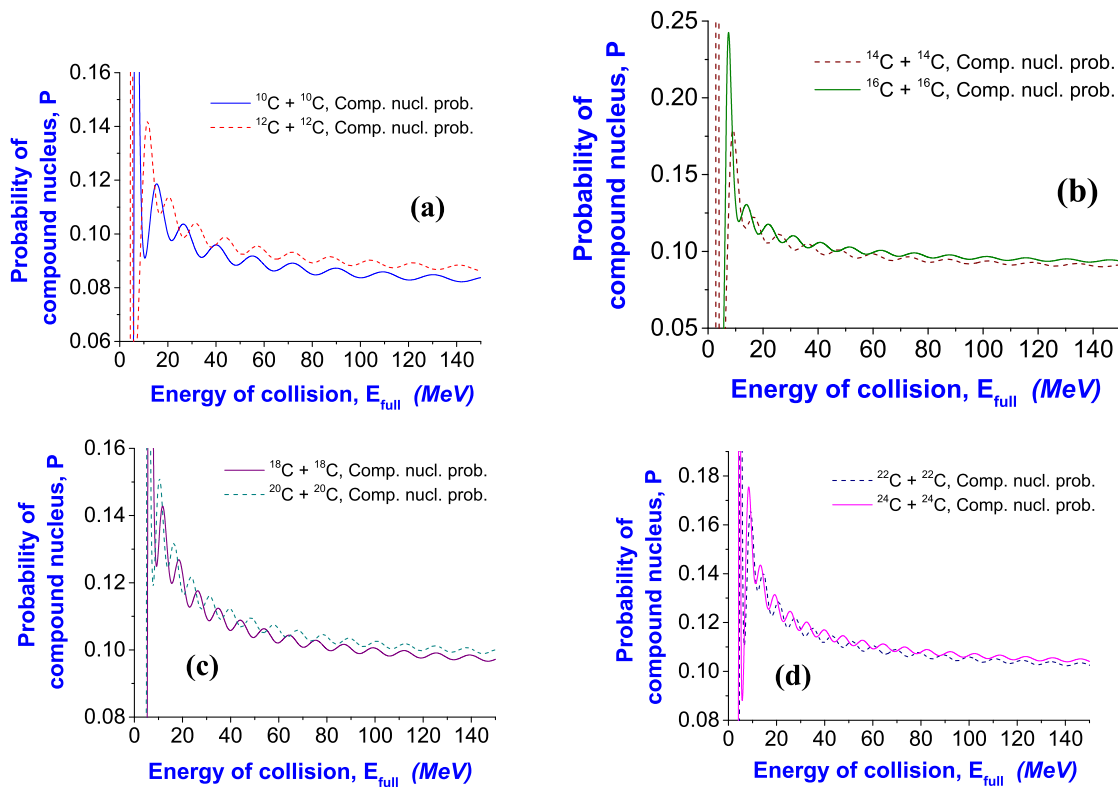


**Figure 2.** Probabilities of formation of a compound nucleus  $P_{cn}$  in dependence on energy for incident isotopes of Carbon in reactions  $^{10}\text{C} + ^{10}\text{C}$ ,  $^{12}\text{C} + ^{12}\text{C}$  (a),  $^{14}\text{C} + ^{14}\text{C}$ ,  $^{16}\text{C} + ^{16}\text{C}$  (b),  $^{18}\text{C} + ^{18}\text{C}$ ,  $^{20}\text{C} + ^{20}\text{C}$  (c), and  $^{22}\text{C} + ^{22}\text{C}$ ,  $^{24}\text{C} + ^{24}\text{C}$  (d) in lattice (potentials and parameters are defined in Equations (19)–(21)). One can clearly see the presence of maxima of such probabilities for all studied isotopes. Energies corresponding to maxima of such probabilities are given in Table 4.

In these figures, one can clearly see the presence of maxima in probabilities at certain definite energies for all studied isotopes of Carbon. This means that at such energies, compound nuclei are formed with maximum probability. Another conclusion from such calculations is that the formation of  $^X\text{Mg}$  nuclei is much more probable at such energies than at energies of zero-mode vibrations. These maxima are explained by strict requirements of quantum mechanics [16], which take into account the further propagation of quantum fluxes in the potential region, in contrast to the existing modern description of pynuclear reactions, where these fluxes are omitted in the nuclear region from the internal turning point.

In Table 4, we present the energies of the quasibound states for reactions with isotopes of Carbon up to 150 MeV.

Only first quasibound energies for  $^{10}\text{C} + ^{10}\text{C}$ ,  $^{12}\text{C} + ^{12}\text{C}$ , and  $^{24}\text{C} + ^{24}\text{C}$  are smaller than the barrier maximums for these nuclear systems. This means that at such energies, compound nuclear systems are the most stable and are transformed to new synthesized isotopes of Magnesium  $^{20}\text{Mg}$ ,  $^{24}\text{Mg}$ , and  $^{48}\text{Mg}$  with large probability. There is a simple way to estimate half-lives of these obtained heavier nuclei using Gamow's approach (well developed in the problem of nuclear decays) or the method of multiple internal reflections for higher precision (we omit these calculations in this paper).

**Table 4.** Energies of the quasibound states of the compound nuclear systems in reactions with isotopes of Carbon  $^{10}\text{C}$ ,  $^{12}\text{C}$ ,  $^{14}\text{C}$ ,  $^{16}\text{C}$ ,  $^{18}\text{C}$ ,  $^{20}\text{C}$ ,  $^{22}\text{C}$ , and  $^{24}\text{C}$ , calculated by the method of multiple internal reflections up to 150 MeV (accuracy of about  $10^{-14}$  in checking test  $|T_{\text{bar}} + R_{\text{bar}}| = 1$  is obtained for each calculation). Comparing these energies with maximums of the potential barriers for all studied systems given in Table 1, we find that only first quasibound energies for  $^{10}\text{C} + ^{10}\text{C}$ ,  $^{12}\text{C} + ^{12}\text{C}$ , and  $^{24}\text{C} + ^{24}\text{C}$  are smaller than barrier maximums for these nuclear systems. That means that at such energies, the compound nuclear systems have barriers that prevent decays from going through the tunneling phenomenon.

No.	$^{10}\text{C} + ^{10}\text{C}$	$^{12}\text{C} + ^{12}\text{C}$	$^{14}\text{C} + ^{14}\text{C}$	$^{16}\text{C} + ^{16}\text{C}$	$^{18}\text{C} + ^{18}\text{C}$	$^{20}\text{C} + ^{20}\text{C}$	$^{22}\text{C} + ^{22}\text{C}$	$^{24}\text{C} + ^{24}\text{C}$
1	0.63471	4.88176	9.06212	7.27054	6.37475	5.47896	5.18036	4.58317
2	15.33267	11.45090	16.52705	13.83968	11.74950	10.55511	9.06212	8.46493
3	26.38076	20.40882	25.78357	21.90180	18.31864	16.52705	14.43687	13.24248
4	40.11623	31.45691	36.23447	30.85972	26.38076	23.69339	20.70741	19.21443
5	55.04609	43.69940	47.58116	40.71343	34.74148	31.15832	27.57515	25.48497
6	71.76754	57.13627	59.82365	51.46293	43.99800	39.51904	35.04008	32.35271
7	89.68337	71.76754	72.96192	62.80962	53.85170	48.47695	42.80361	39.81764
8	109.39078	87.29459	86.99599	74.75351	64.30261	57.73347	51.16433	47.58116
9	130.29259	104.01603	101.62725	87.59319	75.35070	67.88577	60.12224	55.64329
10	–	121.93186	117.45291	101.03006	86.99599	78.03808	69.37000	64.30261
11	–	–	134.17435	115.36273	98.93988	89.08617	79.23246	72.96192
12	–	–	–	130.29259	112.07816	100.43287	89.08617	82.51703
13	–	–	–	146.11824	125.21643	112.37675	99.83567	92.07214
14	–	–	–	–	139.25050	124.91784	110.88377	102.22445
15	–	–	–	–	–	137.75752	122.23046	112.67535
16	–	–	–	–	–	–	134.17435	123.42485
17	–	–	–	–	–	–	146.11824	134.77154
18	–	–	–	–	–	–	–	146.11824

#### 4. Plasma Screening in Nuclear Reactions

It is well known that nuclear reactions at high densities of matter in compact stars are essentially modified due to plasma screening effects [1]. Therefore, a natural question appears as to how many of the results presented above are changed after taking effects of plasma screening into account. We will follow Ref. [10], where effects of plasma screening in thermonuclear fusion reactions in dense nuclear matter in stars were studied. Here, in addition to physical analysis, the authors provided a clear formalism for use and implementations into other research. Therefore, we will estimate the influence of plasma screening on pycnonuclear reactions on the basis of isotope  $^{12}\text{C}$ , and we use that research as a basis for our analysis.

The methodology of the influence of electron clouds on the studied nuclear process is presented in Ref. [10], and we follow this approach. In frameworks of model [10], nuclear reactions are studied under the influence of strong plasma screening. At the first stage, authors introduce the Coulomb potential for colliding nuclei in the standard form as  $U_C(r) = Z_1 Z_2 e^2 / r - H(r)$ , where  $H(r)$  is the mean-field plasma screening potential and  $Z_i$  is the electric charge of the nucleus with the number  $i$  ( $i = 1, 2$ ). Potential  $H(r)$  is determined by the ion-sphere model proposed by Salpeter [23].

$H(r)$  is produced by an electron cloud near nuclei (ions) (see Onsager molecules, e.g., Ref. [24], references therein). Following model [10], the electron cloud is considered as an incompressible uniformly charged liquid drop. This drop has a constant volume, but variable shape. The charge of this drop fully compensates for the charge of the interacting nuclei. The electron drop acts as a Wigner–Seitz cell with tunneling ions.

In the approach of [10], the authors also calculate the astrophysical  $S$ -factors and the reaction rates for thermonuclear reactions by including the screening potential in the total potential. The new modified  $S$ -factor is determined not only by nuclear interactions but also by parameters of dense matter. With the estimation of new rates, the authors found factors of the plasma screening enhancement.

Following Ref. [10] (see Equation (7) in that paper), we define the Coulomb potential  $U_C(r)$  for colliding nuclei in the standard form:

$$U_{C,full}(r) = v_C(r) + H(r), \tag{36}$$

where  $v_C(r)$  is the pure Coulomb potential without screening and  $H(r)$  is the mean-field plasma screening potential. In contrast to Ref. [10], we calculate the pure Coulomb potential  $v_C(r)$  on the basis of Equations (20)–(22) (here, the Coulomb potential in the nuclear region at  $r < R_C$  is different from the corresponding potential in Equation (7) in Ref. [10]), and we use nuclear potential  $v_N(r)$  in Equation (20) (we set  $l = 0$ ). In definition of the screening part of potential, we follow Ref. [10] and use (see Equations (10) and (11) in that paper):

$$H(r) = E_{12} h(x), \quad x = \frac{r}{a_{12}}, \tag{37}$$

where:

$$h(x) = b_0 + b_2 x^2 + b_4 x^4 + \dots \tag{38}$$

At  $Z_1/Z_2 = 1$ , parameters  $b_0$ ,  $b_2$ , and  $b_4$  are derived in Ref. [10] as:

$$b_0 = 1.0573, \quad b_2 = -0.25, \quad b_4 = 0.0394. \tag{39}$$

Other parameters are (see Equations (2) and (4) in Ref. [10]):

$$a_e = \left( \frac{3}{4\pi n_e} \right)^{1/3}, \quad a_j = Z_j^{1/3} a_e, \tag{40}$$

$$a_{12} = \frac{a_1 + a_2}{2}, \quad E_{12} = \frac{Z_1 Z_2 e^2}{a_{12}}, \tag{41}$$

where  $n_e$  is concentration of electrons.

On the basis of Equation (25), we calculate the concentration of nuclei  $n_A$  at the studied density as:

$$^{12}\text{C} + ^{12}\text{C}, \quad \rho_0 = 6 \times 10^9 \frac{\text{g}}{\text{cm}^3} : \quad n_A = 3.01418 \times 10^{-7} \text{ fm}^{-3}. \tag{42}$$

This can be understood as each  $^{12}\text{C}$  nucleus having size of about 200 fm in volume. From here, we find the concentration of electrons:

$$n_e = Z \cdot n_A, \quad n_e = 1.80851 \times 10^{-6} \text{ fm}^{-3} \tag{43}$$

and from Equations (38) and (39), we obtain:

$$a_{12} = 92.52241 \text{ fm}. \tag{44}$$

As it is indicated in Ref. [10], Equation (38) should be used at  $x \ll 2$ . We estimate that this condition is fulfilled in the full region of study of reaction  $^{12}\text{C} + ^{12}\text{C}$  at the chosen density, so we use Equation (38) for the description of the screening part of the potential.

The potential of interactions taking into account screening, calculated by such an approach, is shown in Figure 3.

From this figure, one can see that the screening does not change the potential much at the density of matter under consideration. Therefore, one can suppose that the screening does not influence essentially the results of quasibound states and energies above. However, energies of zero-point vibrations are essentially smaller than quasibound energies, and one can suppose that the energy spectrum of zero-point vibrations will be changed after the inclusion of plasma screening in calculations.

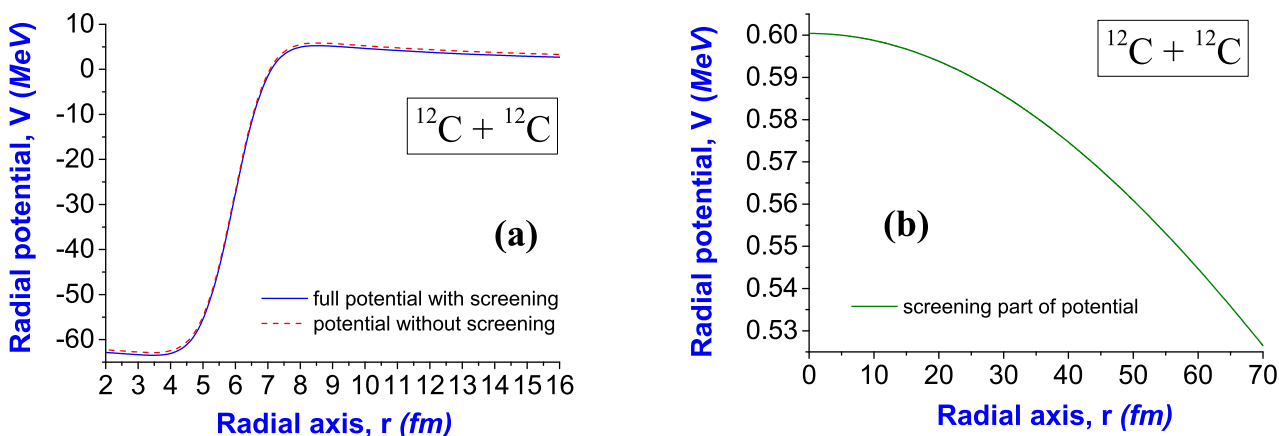


**Figure 3.** Potential of interaction between two  $^{12}\text{C}$  nuclei with the inclusion of screening in comparison with the same potential without screening (a) and the part of the potential describing screening (b) (the potential and parameters are defined in Equations (19)–(21), and the screening part of the potential is defined in Equations (36)–(38)).

In Table 5, values of energies of zero-point vibrations calculated for the reaction  $^{12}\text{C} + ^{12}\text{C}$  are presented with and without taking into account screening.

**Table 5.** Energies for zero-point vibrations  $E_{\text{zero}}^{(\text{mir})}$  (values are presented in MeV, below 5 MeV) calculated for the reaction  $^{12}\text{C} + ^{12}\text{C}$ .

No.	$^{12}\text{C} + ^{12}\text{C}$ with Screening	$^{12}\text{C} + ^{12}\text{C}$ without Screening
1	0.209619238476954	0.517434869739479
2	0.267334669338677	0.536673346693387
3	0.344288577154309	0.546292585170341
4	0.478957915831663	0.555911823647295
5	0.786773547094188	0.575150300601202
6	2.21042084168337	0.594388777555110
7	3.83607214428858	0.613627254509018
8		0.642484969939880
9		0.680961923847695
10		0.729058116232465
11		0.806012024048096
12		0.911823647294589
13		1.11382765531062
14		2.76833667334669
15	—	4.08617234468938

From this table, one can see that the energy spectrum of the zero-point vibrations for the reaction  $^{12}\text{C} + ^{12}\text{C}$  is modified essentially after taking plasma screening into account.

**5. Influence of Vibration of External Nuclei on Calculation of Quasibound States**

Vibrations of the nucleus can be understood as oscillations of the particle inside the potential well in quantum mechanics (for example, see Ref. [16], p. 91). Here, the harmonic oscillator provides a clear example. The ground energy level of this particle inside the potential of the harmonic oscillator is not zero (excited energy levels are also not zero) due to the quantum nature of this phenomenon. Non-zero frequencies correspond to such energies. At the same time, quantum mechanics provides a formalism to calculate the most probable location of this particle, which is at the coordinates of the minimum of the potential well. This picture corresponds to the most probable position of the studied nucleus with non-zero frequencies (i.e., the position of nucleus is fixed in general logic). In other words, vibrations of the nucleus (inside some external field) can be studied in quantum mechanics as a

particle oscillating inside the potential well, and quantum mechanics provides a formalism to calculate non-zero frequencies and the most probable location of this particle.

If we consider the nucleus to be between the two closest nuclei (we will call them “external nuclei”), one can find that this nucleus is located inside the Coulomb fields of the external nuclei. The summation of the Coulomb potentials of the external nuclei gives the harmonic oscillator enough of a small middle region between the external nuclei, which is the approximation for full potential (where we neglect interactions with external nuclei at closer distances). In such a way, we obtain a picture of the oscillation of the particle inside the harmonic potential well, and we report the vibrations of the corresponding nucleus.

However, we should be reminded that nuclear interactions of nuclei exist, which influence the phenomenon described above. In particular, this is crucial in the study of nuclear scattering. From our experience, the role of the nuclear part of the potentials is increased at low energies (this is the case of pycnonuclear reactions). Therefore, we obtain motivation to take into account the influence of nuclear forces from the external nuclei on the process of oscillation of the middle nucleus (the particle inside the more complex potential well, which continues to exist).

After the inclusion of the nuclear parts of the potentials from external nuclei, we obtain two additional (more deep) wells outside the well of harmonic oscillator type. Now, potential barriers appear, and there is a possibility to transfer a particle through any barrier with not-zero probability. This is estimated on the basis of penetrability, which we calculate with high precision, and we propose tests to check the calculations by other researchers. In addition, we find that after tunneling (or transferring the region of the barrier at above-barrier energies), the joint nuclear system (from the middle nucleus and one external nucleus) can exist with higher probability, which we describe and estimate via the formalism of quasibound states.

If we study the interaction of the middle nucleus with one external nucleus, quantum mechanics provides a strict formalism, where the particle with reduced mass moves in the external potential (for example, see Ref. [16], pp. 133–136). The vibrating effects of both nuclei are included in such a model, which can be studied via estimation of energy levels, frequencies, properties of the wave function of this particle, etc. The influence of the second external nucleus can be included also as correction with the addition of a second potential with a second barrier.

However, outside such a correction above, more self-consistent study of joint vibrations of all external nuclei and the middle nucleus can be performed as the next step in this research line (this is a three-body problem in quantum mechanics). This study is omitted in the current manuscript.

## 6. Conclusions and Perspectives

The question of conditions needed for the most probable formation of compound nuclei (as the first stage needed for the synthesis of more heavy elements) in pycnonuclear reactions in compact stars is investigated in this paper. The method is based on the formalism of multiple internal reflections, constructed for the study of quantum phenomena with details, high precision, and tests in nuclear decays [12,19,20] and nuclear captures by nuclei [13,14]. In this paper, we continue investigations of pycnonuclear reactions with isotopes of Carbon, started in Ref. [17] for  $^{12}\text{C} + ^{12}\text{C}$ . Conclusions of our analysis are the following.

- In this research, pycnonuclear processes are studied, taking the nuclear part of the potential of interactions between nuclei into account. The requirement of continuity of quantum flux (describing pycnonuclear reactions on the basis of quantum mechanics) gives new states in which the compound nuclear system of  $^{2X}\text{Mg}$  is formed with the highest probability (see Figure 2). Following the logic in Refs. [13,14,17], we call such states *quasibound states in pycnonuclear reactions*. Note that these states have not been studied yet by other researchers in the study of the synthesis of elements in stars.

- As shown in Figure 2, the probability of formation of a compound nuclear system in quasibound states is essentially higher than the probability of formation of this system in states of zero-point vibrations studied by Zel'dovich [5] and followers of that idea. The synthesis of more heavy nuclei of Magnesium from isotopes of Carbon is essentially more probable in quasibound states than in states of zero-point vibrations. This leads to the revision (reconsideration) of pictures of the formation of heavy elements in compact stars to use quasibound states as the basis for synthesis. Note the perspective to study in more detail the method in this paper on the basis of experimental measurements in Ref. [25].
- Only the first quasibound energies for  $^{10}\text{C} + ^{10}\text{C}$ ,  $^{12}\text{C} + ^{12}\text{C}$ , and  $^{24}\text{C} + ^{24}\text{C}$  (see Table 4) are smaller than the barrier maximums for these nuclear systems (see Table 1). Therefore, at such energies, the compound nuclear systems have barriers that prevent their decays from going through the tunneling phenomenon. At such energies, the compound nuclear systems are the most probable and the most long lived. These systems are transformed into new synthesized isotopes of Magnesium  $^{20}\text{Mg}$ ,  $^{24}\text{Mg}$ , and  $^{48}\text{Mg}$  with large probabilities. There is a simple way to estimate the half-lives of these obtained more heavy nuclei using Gamow's approach or the method of multiple internal reflections for higher precision. Note that other approaches cannot estimate the quasibound energies needed for the prediction of the synthesis of more stable nuclear systems by such a way described above. At the same time, the method of multiple internal reflections calculates such energies with high precision, also providing tests to check calculations. However, the analysis of binding energies for the obtained isotopes of Magnesium shows that only  $^{24}\text{Mg}$  will be stable after synthesis.
- For the first time, the influence of plasma screening on quasibound states and states of zero-point vibrations in pycnonuclear processes has been studied. It is found that the energy spectrum of zero-point vibrations is essentially modified after taking plasma screening into account (see Table 5 for the reaction  $^{12}\text{C} + ^{12}\text{C}$ ).

**Author Contributions:** Conceptualization, S.P.M.; Methodology, S.P.M.; Software, S.P.M. and K.A.S.; Validation, G.W.; Formal analysis, G.W. and K.A.S.; Investigation, S.P.M. and G.W.; Writing—original draft, S.P.M.; Writing—review & editing, G.W.; Funding acquisition, G.W. All authors have read and agreed to the published version of the manuscript.

**Funding:** G.W. and S.P.M. thank the support of OTKA grant K138277.

**Data Availability Statement:** All data in Tables and Figures in this paper are calculated on the basis of the method described in this paper. Formalism of method is presented in short form. But there are citations in reference list where one can find more details about method, its tests, applicability to different tasks, history of developments in such a research line.

**Acknowledgments:** S.P.M. thanks the Wigner Research Centre for Physics in Budapest for warm hospitality and support. Authors are highly appreciative to V. S. Vasilevsky for fruitful discussions concerning mechanisms of formation of the compound nuclear system and scattering of nuclei and peculiarities of the method of multiple internal reflections, A. G. Magner for fruitful discussions concerning the aspects of nuclear matter in conditions of compact stars and in Earth, and V. Ambrus for fruitful discussions concerning physical issues of astrophysical S-factors and applicability of quantum methods in stars.

**Conflicts of Interest:** The authors declare no conflict of interest.

## References

1. Salpeter, E.E.; Horn, H.M.V. Nuclear reaction rates at high densities. *Astrophys. J.* **1969**, *155*, 183.
2. Schramm, S.; Koonin, S.E. Pycnonuclear Fusion Rates. *Astrophys. J.* **1990**, *365*, 296; Erratum in *Astrophys. J.* **1991**, *377*, 343. [[CrossRef](#)]
3. Haensel, P.; Zdunik, J.L. Equation of state and structure of the crust of an accreting neutron star. *Astron. Astrophys.* **1990**, *229*, 117; Erratum in *Astron. Astrophys.* **2003**, *404*, L33.
4. Cameron, A.G.W. Pycnonuclear reactions and nova explosions. *Astrophys. J.* **1959**, *130*, 916. [[CrossRef](#)]
5. Zel'dovich, Y.B.; Guseynov, O.H. Collapsed stars in binaries. *Astrophys. J.* **1965**, *144*, 840. [[CrossRef](#)]

6. Shapiro, S.L.; Teukolsky, S.A. *Black Holes, White Dwarfs, and Neutron Stars: The Physics of Compact Objects*; Wiley: Weinheim, Germany, 2004; 645p.
7. Yakovlev, D.G.; Gasques, L.R.; Beard, M.; Wiescher, M.; Afanasjev, A.V. Fusion reactions in multicomponent dense matter. *Phys. Rev. C* **2006**, *74*, 035803.
8. Beard, M.; Afanasjev, A.V.; Chamon, L.C.; Gasques, L.R.; Wiescher, M.; Yakovlev, D.G. Astrophysical S factors for fusion reactions involving C, O, Ne, and Mg isotopes. *At. Data Nucl. Data Tables* **2010**, *96*, 541–566.
9. Afanasjev, A.V.; Beard, M.; Chugunov, A.I.; Wiescher, M.; Yakovlev, D.G. Large collection of astrophysical S-factors and its compact representation. *Phys. Rev. C* **2012**, *85*, 054615.
10. Kravchuk, P.A.; Yakovlev, D.G. Strong plasma screening in thermonuclear reactions: Electron drop model. *Phys. Rev. C* **2014**, *89*, 015802.
11. Gasques, L.R.; Afanasjev, A.V.; Aguilera, E.F.; Beard, M.; Chamon, L.C.; Ring, P.; Wiescher, M.; Yakovlev, D.G. Nuclear fusion in dense matter: Reaction rate and carbon burning. *Phys. Rev. C* **2005**, *72*, 025806.
12. Maydanyuk, S.P.; Belchikov, S.V. Calculations of penetrability of barriers in the proton decay problem: The fully quantum approach and initial condition of decay. *J. Phys. Stud.* **2011**, *14*, 40.
13. Maydanyuk, S.P.; Zhang, P.-M.; Belchikov, S.V. Quantum design using a multiple internal reflections method in a study of fusion processes in the capture of alpha-particles by nuclei. *Nucl. Phys. A* **2015**, *940*, 89–118.
14. Maydanyuk, S.P.; Zhang, P.-M.; Zou, L.-P. New quasibound states of the compound nucleus in  $\alpha$ -particle capture by the nucleus. *Phys. Rev. C* **2017**, *96*, 014602.
15. Eberhard, K.A.; Appel, C.; Bangert, R.; Cleemann, L.; Eberth, J.; Zobel, V. Fusion cross sections for  $\alpha + {}^{40,44}\text{Ca}$  and the problem of anomalous large-angle scattering. *Phys. Rev. Lett.* **1979**, *43*, 107–110.
16. Landau, L.D.; Lifshitz, E.M. *Kvantovaya Mehanika, Kurs Teoreticheskoi Fiziki (Quantum Mechanics, Course of Theoretical Physics)*; Nauka Publishing: Moscow, Russia, 1989; Pergamon: Oxford, UK, 1982; Volume 3, p. 768. (In Russian)
17. Maydanyuk, S.P.; Shaulskyi, K.A. Quantum design in study of pycnonuclear reactions in compact stars: Nuclear fusion, new quasibound states and spectroscopy. *Eur. Phys. J.* **2022**, *A58*, 220.
18. Chien, L.H.; Khou, D.T.; Cuong, D.C.; Phuc, N.H. Consistent mean-field description of the  ${}^{12}\text{C} + {}^{12}\text{C}$  optical potential at low energies and the astrophysical S factor. *Phys. Rev. C* **2018**, *98*, 064604.
19. Olkhovsky, V.S.; Maydanyuk, S.P. Method of multiple internal reflections in description of tunneling evolution through barriers. *Ukr. Phys. J.* **2000**, *45*, 1262–1269.
20. Maydanyuk, S.P.; Olkhovsky, V.S.; Zaichenko, A.K. The method of multiple internal reflections in description of tunneling evolution of nonrelativistic particles and photons. *J. Phys. Stud.* **2002**, *6*, 1–16.
21. Hamada, T.; Salpeter, E.E. Models for zero-temperature stars. *Astrophys. J.* **1961**, *134*, 683.
22. Maydanyuk, S.P.; Olkhovsky, V.S.; Mandaglio, G.; Manganaro, M.; Fazio, G.; Giardina, G. Bremsstrahlung emission of high energy accompanying spontaneous of  ${}^{252}\text{Cf}$ . *Phys. Rev. C* **2010**, *82*, 014602.
23. Salpeter, E.E. Electron screening and thermonuclear reactions. *Aust. J. Phys.* **1954**, *7*, 373. [[CrossRef](#)]
24. Rosenfeld, Y.; Chabrier, G. Onsager molecules for the Yukawa potentials: Screening potentials and the Jancovici coefficient in strongly coupled electron-screened plasmas. *J. Stat. Phys.* **1997**, *89*, 283.
25. Fang, X.; Tan, W.P.; Beard, M.; deBoer, R.J.; Gilardy, G.; Jung, H.; Liu, Q.; Lyons, S.; Robertson, D.; Setoodehnia, K.; et al. Experimental measurement of  ${}^{12}\text{C} + {}^{16}\text{O}$  fusion at stellar energies. *Phys. Rev. C* **2017**, *96*, 045804.

**Disclaimer/Publisher's Note:** The statements, opinions and data contained in all publications are solely those of the individual author(s) and contributor(s) and not of MDPI and/or the editor(s). MDPI and/or the editor(s) disclaim responsibility for any injury to people or property resulting from any ideas, methods, instructions or products referred to in the content.